Flow Behavior in a Corotating Twin-Screw Extruder of Pure Polymers and Blends: Characterization by Fluorescence Monitoring Technique

Haixia Fang,[1,2] Frej Mighri,[1,2] Abdellah Ajji,[1,3] Philippe Cassagnau,[4,5] Said Elkoun[1,6]

[1]*CREPEC, Center for Applied Research on Polymers and Composites, Montreal, Quebec, Canada*
[2]*Department of Chemical Engineering, Laval University, Quebec, Canada G1K 7P4*
[3]*Department of Chemical Engineering, Ecole Polytechnique of Montreal, Quebec, Canada H3T 1J4*
[4]*Laboratoire des Matériaux (Université de Lyon 1), Lyon, F-69003 France*
[5]*Laboratoire des Matériaux Polymères et Biomatériaux, F-69622 Villeurbanne, France*
[6]*Department of Mechanical Engineering, Sherbrooke University, Quebec, Canada J1K 2R1*

Received 9 March 2010; accepted 19 September 2010
DOI 10.1002/app.33414
Published online 10 December 2010 in Wiley Online Library (wileyonlinelibrary.com).

ABSTRACT: The objective of this work was to investigate the flow behavior of pure polymers and blends, especially miscible polymer/polymer systems, in a corotating twin-screw extruder (TSE) using an online fluorescence monitoring device. An immiscible blend was also studied for the sake of comparison. The fluorescence signal was obtained by using synthesized fluorescence tracers added to the melt at very low concentrations. These tracers consisted of two styrene-maleic anhydride copolymers (SMA) labeled with anthracene. The investigated blends were SMA8 (8 wt % of MA in SMA)/polystyrene (PS), SMA14 (14 wt % of MA in SMA)/styrene acrylonitrile copolymer (SAN), and poly(methyl methacrylate) (PMMA)/ethyl acrylate-methyl methacrylate copolymer (PMMAEA). The residence time distribution (RTD), the mean residence time ($\bar{t}$), the dimensionless variance (σ_θ^2), the Peclet number (*Pe*) and the fluorescence peak intensity distribution of pure polymers and binary polymer systems were investigated and interpreted in terms of polymers rheological properties. It was observed that polymers presenting higher viscosity or higher pressure showed longer residence time. A difference in behavior was also observed for the RTD of miscible and immiscible blends.
 J Appl Polym Sci 120: 2304–2312, 2011

Key words: fluorescence; residence time distribution; mean residence time; twin-screw extrusion; blend miscibility

INTRODUCTION

The residence time distribution (RTD) of a polymer or a polymer blend inside a twin-screw extruder (TSE) depicts its mixing history along the extruder screws. Being a direct measure of the polymer or the polymer blend mixing quality, the RTD is a crucial parameter that can be used to scale-up and improve screw design and optimize the TSE processing conditions. It allows also reaching perfect polymer mixing or perfect dispersion of additives and fillers inside a polymer matrix. The RTD generally involves the injection of a tracer as a pulse at the TSE feeding hopper, together with the virgin or filled polymers to be characterized. Many techniques have been developed to measure the RTD using different kinds of tracers.[1–7] Among these techniques, online fluorescence, which consists in introducing a fluorescent tracer into the melt, has been applied for monitoring RTDs during melt extrusion. This technique is known for its high signal sensitivity at low tracer concentrations. It can also use macromolecular tracers incorporated in a polymer matrix of approximately the same rheological properties as those of the monitored material. Their low weight concentration, generally less than 0.001 wt %, has no measurable effect on flow behavior.

To measure accurately the RTD, the tracer should have the same flow behavior as the investigated polymer melt. Cassagnau et al.[8] grafted poly(vinyl chloride) (PVC) with anthracene and phenyl to measure the RTD of PVC in TSE with corotating and counter-rotating configurations. They observed that the synthesized macrotracer presented shorter mean residence time and narrower distribution compared with the RTD measured with free anthracene

Correspondence to: F. Mighri (frej.mighri@gch.ulaval.ca).
Contract grant sponsors: "Le Fonds Québécois de la Recherche sur la Nature et les Technologies" (FQRNT), Natural Sciences and Engineering Research Council of Canada (NSERC).

microtracer. The same observation was also reported by Lappe and Potente[9] and Weiss and Stamato.[10] However, Hu and Kadri[3] and Kadri[11] reported that RTD measured for different polymer systems was not influenced by the type of tracer used. In their study, they prepared macrotracers that are compatible with the polymer systems investigated. For example, for polystyrene (PS) and poly(methyl methacrylate) (PMMA), the macrotracers were antracene-bearing PS and antracene-bearing PMMA, which were used to determine the RTD functions in the TSE of PS and PMMA. Those RTDs were then compared with those obtained using free anthracene as microtracer. No visible difference was observed between the RTDs measured using the microtracer or the macrotracer. Although the small molecule microtracer had different rheological properties than those of the polymer matrix, it still yielded the same RTD curve as the macrotracer if it was well dispersed at very small amounts in the matrix (its self-diffusion over the extruder should be negligible).

Generally, the RTD of pure polymers in TSE was widely investigated.[4,12–16] Its variation as a function of processing parameters, geometry of the equipment, and polymer properties (such as shear or extensional viscosity, elasticity, etc.) is largely understood. For example, an increase in the feeding rate reduces the mean residence time and lowers the mixing performance, while an increase of the screw rotation speed reduces the mean residence time, but enhances the axial dispersion.[4] Mean residence time and mixing performance are increased for screw profiles with kneading blocks or left handed screw elements.[12] The study of Zhang et al.[17,18] characterized the mean residence time and the axial mixing quality in a kneading zone composed of kneading discs of various staggering angles. It showed that the axial mixing performance was improved with increasing the staggering angle. The best mixing quality was obtained for a staggering angle of 90°. The authors also showed that gear blocks performed better axial mixing than kneading blocks. Comparative measurements of RDT for low-density polyethylene (LDPE) and linear low-density polyethylene (LLDPE) revealed that LDPE had a narrower RTD and lower axial mixing than LLDPE because of its higher extensional viscosity.[13] Elkouss et al.[14] studied the RTD for binary polymer blends with different and relatively similar viscosities. They showed that, for relatively similar viscosity systems, the two polymers had very different RTD behavior. On the other hand, two polymers having different viscosities displayed similar RTD. They showed that the characteristic relaxation time (elasticity) of the polymer had a crucial effect on the RTD and this effect depended on extrusion parameters. Kao and Allison[15] found that a change in barrel temperature had no significant effect on RTD for styrene copolymer in a TSE. On the contrary, Tzoganakis et al.[16] observed that, for single-screw extrusion process, the RTD breadth for polypropylene (PP) decreased slightly with increasing barrel temperature by 10°C. The reduction in melt viscosity resulting from temperature change increased the drag flow, thus leading to less back mixing along the extruder barrel. However, it was observed that RTD breadth of PP was increased when peroxide-initiated degradation reaction occurred. This increase was attributed to PP degradation, which caused an important reduction in PP melt viscosity and favored pressure-driven back flow.

Our literature review shows that only few studies were performed on RTD of polymer blends. Cassagnau et al.[19] studied the RTD behavior in TSE of two binary systems having large differences in viscosity: ethylene and vinyl acetate copolymer (EVA)/bis(2-ethylhexyl)phthalate (DOP) and EVA/ethylene-glycol (EG). The RTD curve of EVA/DOP system showed the same breadth as EVA and shifted slightly to shorter times with increasing the flow rate. For EVA/EG system, the EG liquid component acted as a lubricant, and the mean residence time was significantly longer at higher flow rate. Kadri[11] measured the RTD of immiscible PS/PMMA blends using synthesized PS and PMMA macrotracers and found that PS and PMMA phases had different mean residence times, especially at low screw rotation speed. This difference, which was minimized by increasing the screw rotational speed, was attributed to the difference in PS and PMMA flow behaviors in the region between the solid conveying and mixing zones because of their different melting speeds.

To the best of our knowledge, no study has been reported on the RTD behavior of miscible polymer blends. The objective of this work was to characterize the RTD of miscible blends, such as styrene-maleic anhydride (SMA)14/styrene acrylonitrile (SAN)17 and PMMAEA/PMMA using the online fluorescence technique. For comparison purpose, an immiscible SMA8/PS blend was also studied using the same technique. The effect of the rheological properties of the polymers on the RTD was also investigated.

EXPERIMENTAL

Materials

All polymers used in this study were commercial grades and had quite close refractive indices to eliminate their influence on light scattering and transmission in the polymer melts.[20] SMA8 and SMA14, having respectively, 8 and 14 wt % of maleic anhydride, were kindly supplied by Arco

TABLE I
Glass Transition Temperature, T_g, Density, and Refractive Index of the Polymers Used

Polymer	Commercial name	T_g(°C)[a]	Density (g/cm^3)[b]	Refractive index[b]
SMA8	Dylark 232	118	1.08	1.58
SMA14	Dylark 332	129	1.11	1.58
SAN17	Sparkle	102	1.07	1.57
PS	PS 667	102	1.04	1.58
PMMA	Plexiglas VM-100	104	1.18	1.49
PMMAEA	Plexiglas V052	92	1.19	1.49

[a] Measured by DSC.
[b] Data from suppliers.

Company, USA. SAN17 (from Lustran Polymers, USA) has 17 wt % of acrylonitrile. PS-101 was purchased from Nova Corp., Canada. 2-Amino anthracene (94%) was purchased from Alfa Company. PMMA (Plexiglas VM-100) and methyl methacrylate-ethyl acrylate copolymer (PMMAEA, Plexiglas V052) were respectively, supplied by Atohaas Americas Inc, USA and Rohm and Haas, USA. The glass transition temperature (T_g), measured by Diffrential Scanning Calorimetry (DSC), density, and refractive indices of the above polymers are listed in Table I. The solvents (xylene, methanol, tetrahydrofuran (THF), and hexane) were GR grade, purchased from EMD chemicals.

SMA-anthracene (SMA-An) tracer synthesis

First, two mixtures of 2-amino anthracene with SMA8 (molar ratio: 2 : 1) and with SMA14 (molar ratio 1 : 1) were prepared. Each mixture was then dissolved in 125 mL of xylene and stirred at 120°C in an oil bath for 8 h. The modified SMA8-An and SMA14-An were then purified by precipitation in methanol, and the solid products were redissolved in THF and reprecipitated in hexane two more times. The two purified polymers were finally dried under vacuum at 70°C for 7 days and then compressed at 180°C to form films of about 1 mm in thickness.

Characterization techniques

The imidization reaction of SMA, illustrated in Scheme 1, was characterized by attenuated total reflectance (ATR). ATR spectra were collected in a Bomem FTLA 2000 instrument at a resolution of 4 cm^{-1} with 16 scans. Dynamic mechanical and thermal analysis (DMTA) of the PMMA/PMMAEA systems was carried out on compression-molded rectangular specimens of $\sim 45 \times 6 \times 1.5$ mm^3 using a Rheometrics Scientific analyzer (RSA II) at a frequency of 1 Hz, a strain of 0.02% and a temperature scanning rate of 2°C/min (from 25°C to 160°C). Melt rheological characterization was performed on compression molded samples using an ARES Rheometer (Rheometrics scientific, USA) with parallel plates of 25 mm in diameter. All frequency sweep tests were performed at 2% strain and a temperature of 205°C, i.e., close to the extrusion temperature at the die.

Twin-screw extrusion process and online fluorescence system

Melt extrusion was performed using a 27 mm Leistritz corotating TSE (ZSE-27). The barrel and die temperature setting profile was kept constant at 200/210/210/210/210/210/200/200/200°C (from rear to front along the barrel zones) and 190°C (at the die). The feeding rate and screws rotational speed were also kept constant at 3 kg/h and 120 rpm, respectively. After a stabilization period (of around 10–15 min from the beginning of the extrusion), a small tracer amount was added, as a pulse input, directly inside the main hopper.

The fluorescence probe (fused-silica optical-fiber) was installed directly on the extruder die inside a standard sensor port normally used for temperature or pressure transducers (Fig. 1). This probe was composed of a bifurcated optical fiber cable with one end enclosed in a stainless-steel shell comporting a sapphire window that protects the fibers from the high pressure of the molten polymer. One branch of the cable contained one optical fiber (0.6 mm in diameter) that carries the excitation light from an ultraviolet light source (100W Xenon) to the extruded resin. The other branch contained twelve fibers (0.2 mm in diameter) that transmit the tracer fluorescence emission to the photomultiplier, from which an amplified analog signal (voltage signal between 0 and 5 V) was collected using a Labview data acquisition system (version 7.1). Signals were collected at a frequency of 12 times per second and the average value of every consecutive 200 signals was retained for analysis. To optimize the rate of data acquisition, only the intensities at specific wavelengths were monitored. This was accomplished by using two band pass filters designated as B in Figure 1. The first (placed at the exit of the Xenon lamp) was centered at 365 ± 12.5 nm

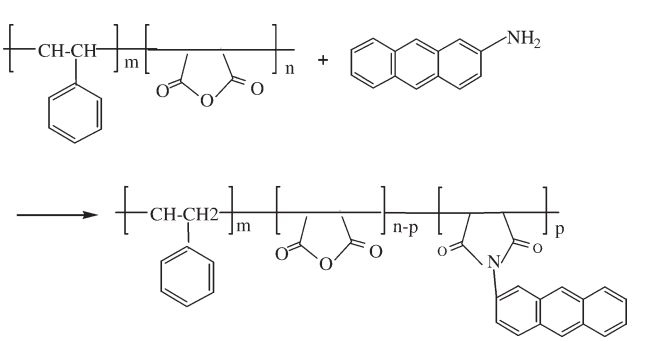

Scheme 1 Scheme of the imidization reaction between SMA and amino-anthracene.

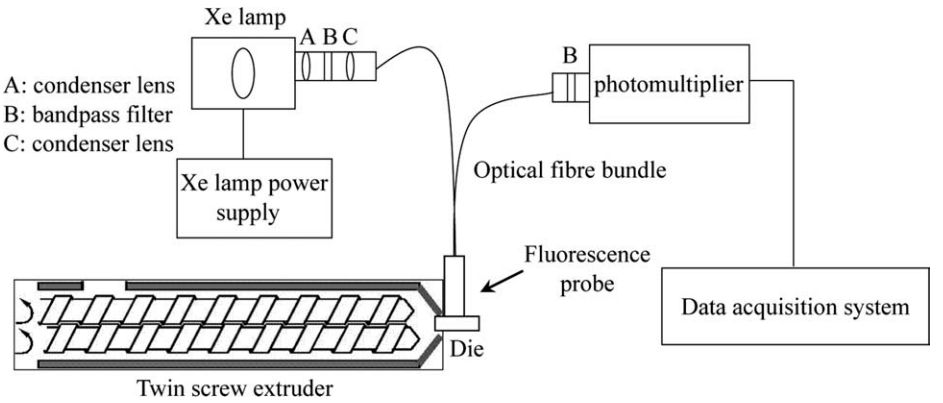

Figure 1 Sketch of the online fluorescence system.

and the second (placed at the entrance of the photomultiplier) was centered at 400 ± 20 nm.

THEORETICAL ASPECTS

As reported by Levenspiel,[21] the normalized RTD density function $E(t)$ can be described as a function of the fluorescence signal $c(t)$, monitored from the moment when the tracer is incorporated at the main hopper of the extruder:

$$E(t) = \frac{c(t)}{\int_0^\infty c(t)dt} = \frac{c(t_i)}{\sum_{i=1}^{n} c(t_i)(t_i - t_{i-1})} \quad (1)$$

where t_i corresponds to the time of signal acquisition ($i = 1,2,3,4,\ldots,n$) and ($t_i - t_{i-1}$) corresponds to the time interval between two consecutive data acquisitions. The mean residence time ($\bar{t}$) along the extruder barrel and the variance of its distribution (σ^2) are given by the following equations:

$$\bar{t} = \int_0^\infty tE(t)dt = \int_0^\infty tc(t)dt \Big/ \int_0^\infty c(t)dt = \sum_{i=1}^{n} t_i c(t_i)(t_i - t_{i-1}) \Big/ \sum_{i=1}^{n} c(t_i)(t_i - t_{i-1}) \quad (2)$$

$$\sigma^2 = \int_0^\infty (t - \bar{t})^2 E(t)dt = \sum_{i=1}^{n} (t_i - \bar{t})^2 E(t_i)(t_i - t_{i-1}) \quad (3)$$

The dimensionless variance (σ_θ^2), which varies between 0 and 1 for real systems, is defined as:

$$\sigma_\theta^2 = \frac{\sigma^2}{(\bar{t})^2} \quad (4)$$

The lower limit of $\sigma_\theta{}^2$ characterizes the ideal plug flow and its higher limit characterizes the perfect mixing flow. Another parameter, the Peclet number (Pe), which is reciprocal to the dispersion number ($D/\mu L$), where D is the diffusivity (m^2/s), μ the velocity (m/s), and L the vessel length (m), characterizes the axial mixing along the extruder. When $D/\mu L$ approaches zero, the dispersion is negligible, resulting in a plug flow. As $D/\mu L$ approaches infinity, the dispersion is important and consequently the flow is mixed. In an extruder, the value of $D/\mu L$ can be calculated from the mean residence time and is related to σ_θ^2 as follows[22]:

$$\sigma_\theta^2 = \frac{2}{Pe} - \frac{2}{Pe^2}(1 - e^{-Pe}) \quad (5)$$

It is obvious from eq. (5) that σ_θ^2, a measure of the axial mixing quality, decreases with increasing Pe.

The following equation gives another form for $\bar{t}$ that shows its relation to the volumetric feeding rate (Q) and screw rotational speed (N)[23,24]:

$$\bar{t} = \frac{A}{Q} + \frac{B}{N} \quad (6)$$

where the two parameters A and B are related to screw geometry and are constant for a given screw configuration. For the same N, $\bar{t}$ decreases with increasing Q. If Q is replaced by the ratio of the mass flow rate (M) and the polymer density (ρ), eq. (6) can be rewritten as follows:

$$\bar{t} = \frac{A \times \rho}{M} + \frac{B}{N} \quad (7)$$

For the same M and N, $\bar{t}$ is proportional to polymer density.

RESULTS AND DISCUSSION

ATR characterization of modified SMA tracer

ATR spectra (in the range of 2000–1500 cm^{-1}) of pure SMA8 and SMA14 copolymers and their

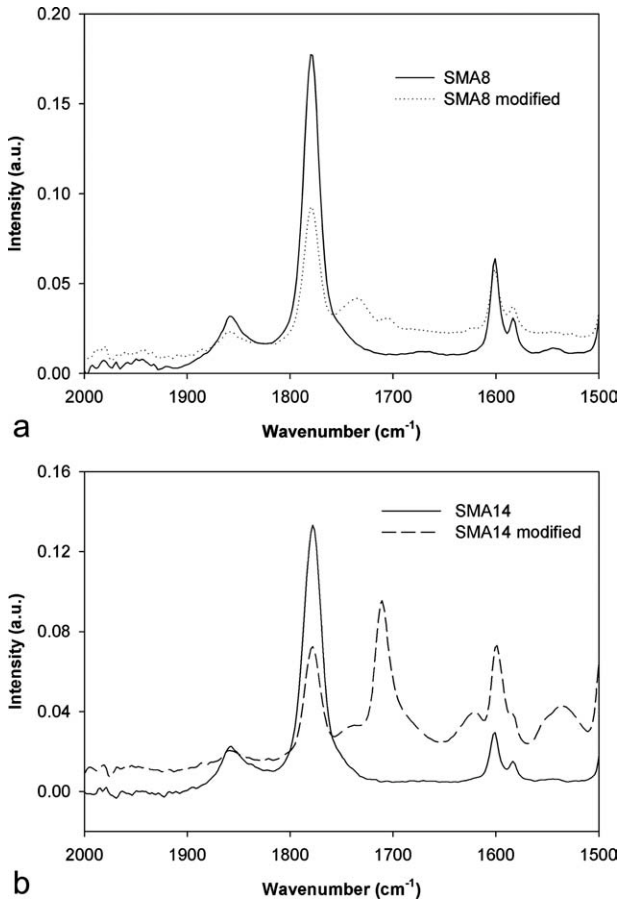

Figure 2 ATR spectra of original and modified SMA8 (a) and SMA14 (b).

corresponding SMA8-An and SMA14-An tracers are presented in Figure 2(a,b), respectively. The carbonyl absorption of anhydride groups in five-membered rings for both original and modified SMA8 and SMA14 corresponds to the peaks at 1780 and 1863 cm^{-1}, respectively. The typical C=C vinyl stretching of styrene corresponds to the peak at 1600 cm^{-1}. Also, the amide ring is completely closed since there is no peak at 1680 cm^{-1}. The conversion from anhydride to imide for SMA tracer was verified by a decrease of 1780 cm^{-1}, and the new signal appearing at 1712 cm^{-1}. The degree of conversion of the imidization reaction, calculated according to Martinez et al.,[25] was 49% for SMA8 and 75% for SMA14.

Assessment of the online fluorescence setup

First, the reproducibility of the RTD measurements and the linearity between the amplitude of the fluorescence signal and the amount of tracer incorporated at the main hopper of the extruder were investigated on molten SMA8 polymer. Figure 3 shows the intensity of the fluorescence signal c (t) (volts) collected at the extruder die as a function of extrusion time t (s) for three runs performed under the same conditions. The amount of SMA8-An tracer was approximately the same for the three runs (0.0423, 0.0432, and 0.0446 g). The figure shows that, for approximately the same tracer concentration, the collected signal was almost the same, which confirms the good reproducibility of the fluorescence signal. In Figure 4(a), $c(t)$ is reported as a function of time at the same extrusion conditions for seven different SMA8-An tracer concentrations (0.0092, 0.0173, 0.0306, 0.0409, 0.0522, 0.0653, and 0.0854 g). The objective of these measurements was to verify the linearity between the fluorescence signal and the amount of SMA8-An tracer. The figure shows that $c(t)$ increases with increasing tracer weight concentration in the melt. It should be noted that the baseline of each curve, which corresponds to the voltage measured at the beginning of signal acquisition (without any signal from SMA8-An tracer), was not zero. All steady-state baselines were then shifted to zero, and the corresponding $c(t)$ were consequently shifted down by the same voltage. Figure 4(b) shows the integrated area over the extrusion time, t, taken from the corrected $c(t)$ curves, as a function of SMA8-An tracer concentration. It can be seen that for all tracer concentrations investigated, the integrated areas were linearly proportional to the tracer concentration and, with adequate calibration, can be used as a measure of tracer concentration in the polymer melt at the die.

When the measured fluorescence signals $c(t)$ for the extruded SMA8 are used in eqs. (2)–(5), the values of the mean residence time ($\bar{t}$), the variance of the distribution (σ^2), and the dimensionless variance (σ_θ^2) can be calculated as a function of tracer concentration. The corresponding results are shown in Figure 5(a) for $\bar{t}$ and σ^2 and Figure 5(b) for σ_θ^2. It is seen from Figure 5(a) that $\bar{t}$ increased from 300 to 367 s and σ^2 increased from 11,044 to 17,600 with

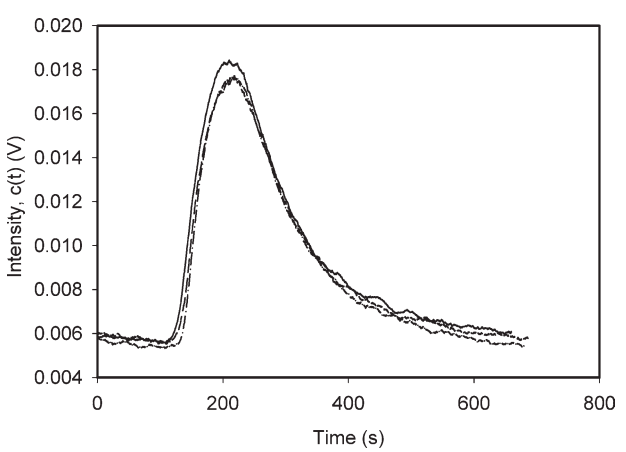

Figure 3 SMA8 fluorescence signal $c(t)$ for three runs under the same extrusion conditions and approximately the same SMA8-An tracer concentration (0.0423, 0.0432, and 0.0446 g).

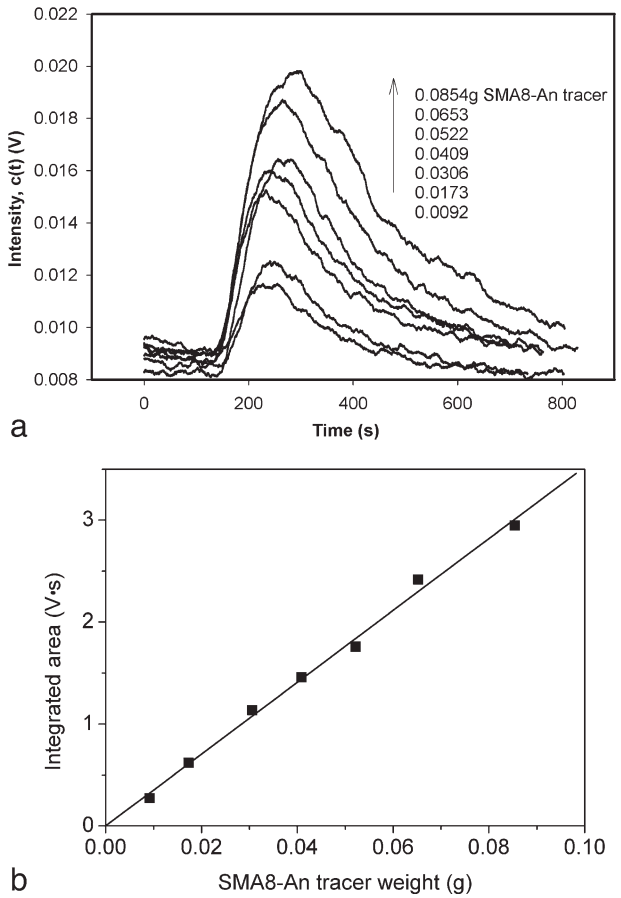

Figure 4 (a) Effect of SMA8-An tracer concentration on the fluorescence signal for SMA8. (b) Linear relationship between the integrated area of RTD curve and SMA8-An tracer concentration.

increasing SMA8-An tracer concentration from 0 to 0.0854 g. The same phenomenon was reported by Lee et al.[26] who monitored the RTD behavior of polyethylene using an ultrasound device and $CaCO_3$ tracer. So, the tracer concentration should be constant when the RTD behavior is measured for different polymers and varying processing conditions. However, Figure 5(b) shows no obvious variation of σ_θ^2 with tracer concentration, which means that the axial mixing quality of the polymer can be monitored effectively by the fluorescence SMA8-An tracer.

Characterization of pure polymers RTD behavior by fluorescence technique

The influence of polymer rheological properties on the RTD behavior was already investigated. Chen et al.[27] found that a polymer with lower viscosity (higher melt flow index) had longer $\bar{t}$, but its axial mixing (dispersion) quality was not affected by viscosity. Polance and Jayaraman[13] revealed that polymers with lower extensional viscosity had shorter $\bar{t}$ and better axial mixing quality. In the present study, we investigated $\bar{t}$ and *Pe* number (the latter being a measure of the axial mixing quality), given by eqs. (2) and (5), respectively, for six polymers of different viscoelastic properties. Polymers complex viscosities at 205°C are shown in Figure 6(a) as a function of frequency. Figure 6(b) shows their corresponding $\bar{t}$ (gray bar) and *Pe* number (hatched bar). As mentioned in the experimental section, the TSE rotational speed was 120 rpm, which means that the extruded polymers were under high average shear rates along the TSE screws. Figure 6(a) shows that at high frequencies, PMMA has lower complex viscosity than PMMAEA. However, as shown in Figure 6(b), it exhibits higher $\bar{t}$ (361 s for PMMA compared to 323 s for PMMEA). This longer $\bar{t}$ for PMMA is mainly attributed to its higher glass transition temperature (104°C) compared with that of PMMAEA (92°C). In addition, we observed that the torque during PMMA extrusion was 5%–10% higher than that measured for PMMAEA. This was because of the delay between PMMA and PMMAEA softening, which is longer for PMMA. Figure 6(c) shows $\bar{t}$ as a function of polymer density for the six polymers studied. In general, $\bar{t}$ was higher for polymers

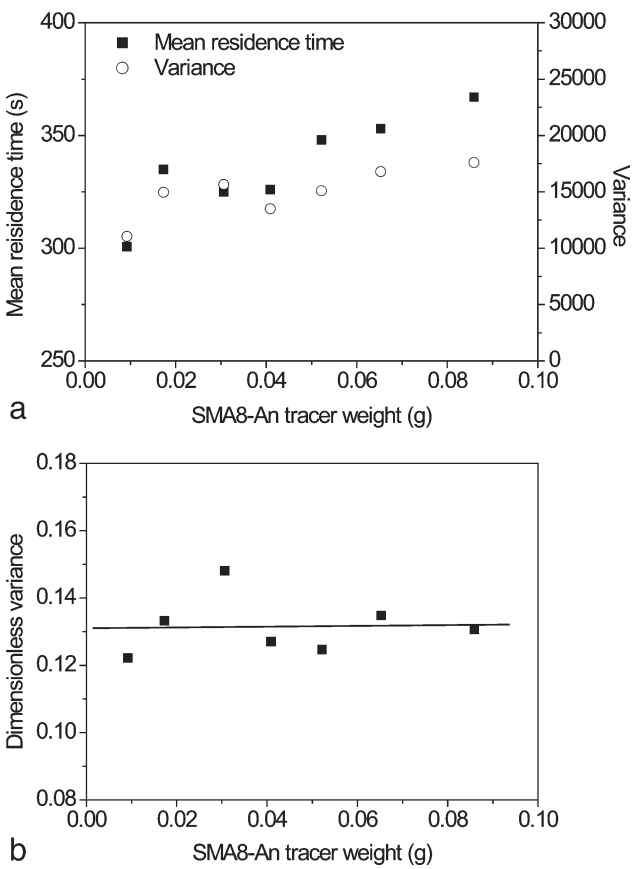

Figure 5 (a) Measured mean residence time $(\bar{t})$ and variance of distribution (σ^2) for SMA8 as a function of SMA8-An tracer concentration. (b) Measured dimensionless variance as a function of tracer concentration.

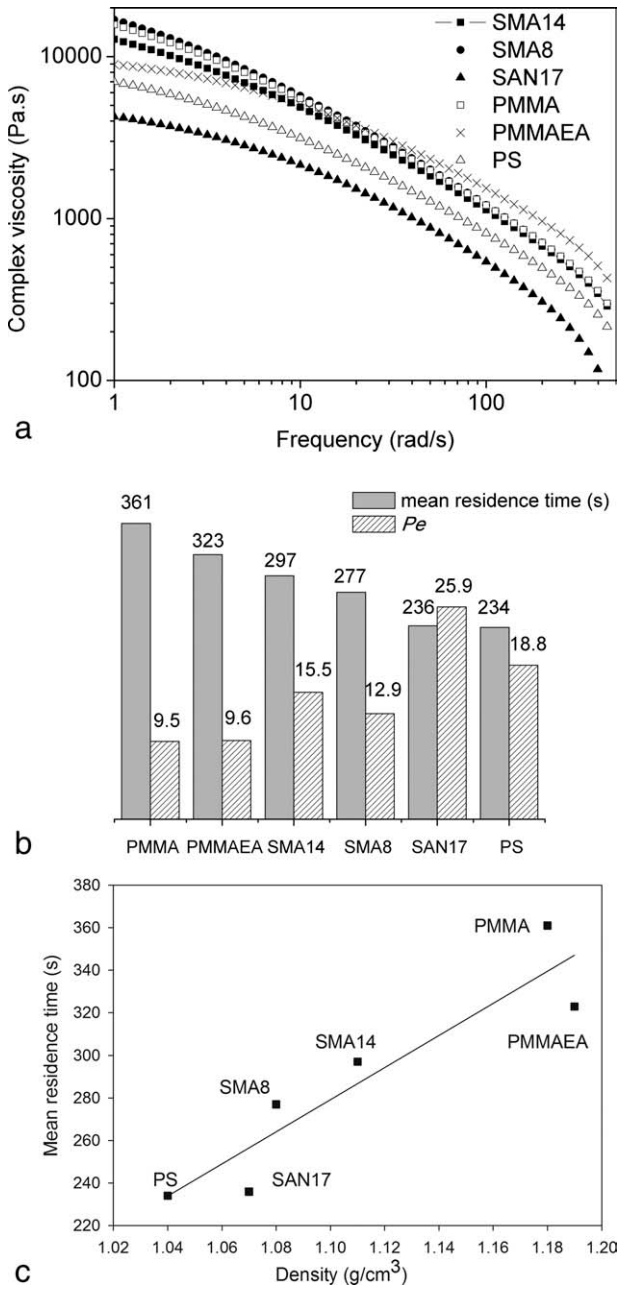

Figure 6 (a) Complex viscosity (at 205°C) as a function of frequency for all the polymers. (b) Mean residence time ($\bar{t}$) and Peclet number (*Pe*) for the different polymers studied. (c) Mean residence time ($\bar{t}$) as a function of polymer density.

of higher densities. However, for PMMA and PMMAEA, which have quite similar densities, their corresponding $\bar{t}$ was quite different. The difference was also observed during PMMA extrusion where the measured torque was 5%–10% higher than that measured for PMMAEA, although PMMA complex viscosity at high frequency was lower than that of PMMAEA. This could be because of the delay between PMMA and PMMAEA softening.

Generally, the six polymers investigated in this study can be classified into the three following families, depending on their rheological or extrusion behaviors: (i) those having the highest melt complex viscosity or the highest melt pressure at the extruder die (PMMA and PMMAEA), (ii) those of intermediate complex viscosity/or melt pressure (SMA8 and SMA14), and (iii) those with the lowest complex viscosity/or melt pressure (SAN17 and PS). The polymers presenting higher melt pressure or higher complex viscosity took longer residence time along the TSE barrel and consequently led to a better axial dispersion.

Miscibility of polymer/polymer blend systems by DMTA

Bikiaris et al.[28] investigated the miscibility of SMA8/PS system by the DMTA technique. For all compositions studied, they observed two glass transitions, a characteristic of an immiscible SMA8/PS system. However, these glass transitions were lower than those of pure SMA8 and PS phases, which indicated a weak interaction between the two phases. As mentioned in literature,[29–31] SMA/SAN systems are miscible when SMA and SAN have similar weight percent of maleic anhydride and acrylonitrile comonomers, respectively. In this study, we characterized the miscibility of PMMAEA/PMMA system by DMTA. Figure 7 shows the loss tangent (tan δ, ratio between viscous and elastic stresses) as a function of temperature for pure PMMAEA and PMMA phases and also for two compositions (80/20 and 40/60). For these two compositions, PMMAEA/PMMA system presented a single T_g (it corresponds to the temperature at the tan δ peak), which is a characteristic of a miscible system. Thus, the incorporation of ethyl acrylate had no influence on the miscibility of

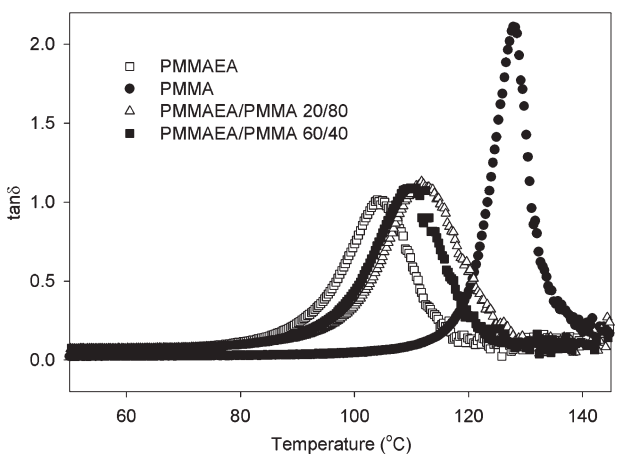

Figure 7 Loss angular, tan δ, as a function of temperature for the PMMA/PMMAEA systems.

PMMAEA with PMMA because of the small polarity difference between MMA and EA groups.

Flow behavior characterization by fluorescence technique for immiscible and miscible systems

The integrated fluorescence intensity taken from the RTD curves for SMA8/PS, SMA14/SAN17, and PMMAEA/PMMA systems of varied compositions are presented in Figure 8(a) as a function of systems composition. The figure shows that the fluorescence intensity for PS is smaller than that of SMA. In the immiscible SMA8/PS blend, the SMA8-An tracer tends to disperse in the SMA8 phase, leading to higher tracer concentration in this phase compared with pure SMA8. Thus, the fluorescence intensity was slightly higher in the SMA8/PS system than in pure SMA8. Due to the similar refractive indices of SMA8 and PS, it was observed that for all the compositions, the SMA8/PS system was transparent despite its immiscibility. For the miscible SMA14/SAN17 system, Figure 8(a) shows that the fluorescence intensity varies almost linearly with system composition. This was also observed in our previous work[32] for the same system prepared by solution casting method. So, this linear variation of the fluorescence intensity peak confirms that SMA14 and SAN17 chains were interpenetrating each other, and consequently, the SMA14-An tracer was homogeneously dispersed in both SMA14 and SAN17 phases. The SMA14-An tracer was also used to measure RTD behavior of PMMAEA/PMMA system. The fluorescence intensity peak also shows a linear variation with system composition, a characteristic of miscible systems. Hence, as in the case of SMA14/SAN17 system, SMA14 tracer was distributed homogeneously in both PMMA and PMMAEA because of their chain interpenetration.

Figure 8(b) shows $\bar{t}$ (measured using SMA8-An and SAM14-An tracers) for the same three systems presented above. For the immiscible SMA8/PS system, $\bar{t}$ was between those of pure SMA8 and PS phases, but closer to that of SMA8. As mentioned above for the fluorescence peak intensity of this system, the preferential localization of SMA8-An tracer was inside the SMA8 phase and, it consequently monitors only the flow behavior of this phase along the TSE. For the miscible SMA14/SAN17 system, Figure 8(b) shows that $\bar{t}$ also varies almost linearly between those of pure SMA14 and SAN17 phases, similar to the fluorescence peak intensity. This indicates that the SMA14-An tracer characterizes the flow behavior of the whole miscible system. As in the case of SMA14/SAN17 system, Figure 8(b) also shows that $\bar{t}$ of the PMMAEA/PMMA system measured by SMA14-An tracer decreased almost linearly between those of PMMA and PMMAEA phases with increasing PMMAEA weight content. Thus, the SMA14-An tracer was randomly distributed in the whole miscible PMMAEA/PMMA system and consequently characterizes the whole system behavior. The figure shows also that the PMMAEA/PMMA (20/80) system had the same residence time as pure PMMA, which indicates that

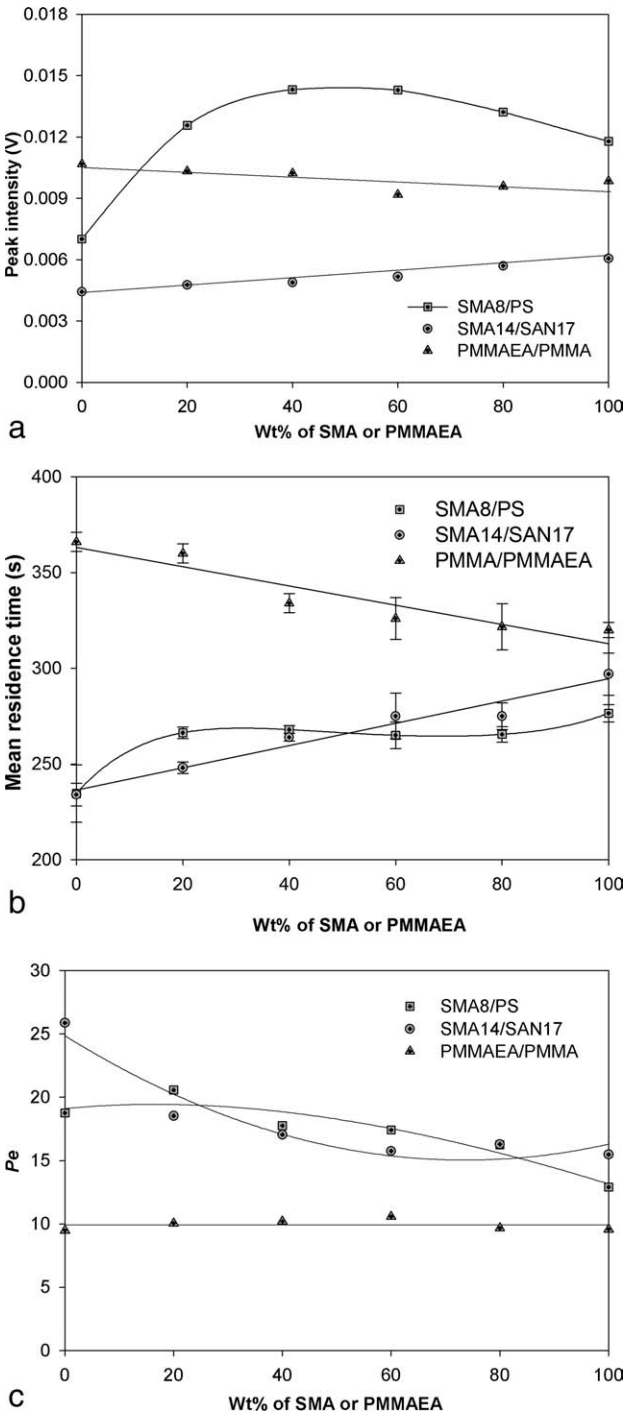

Figure 8 (a) Fluorescence intensity variation with composition in the blends. (b) Mean residence time $(\bar{t})$ variation with composition in the blends. (c) Peclet number (Pe) variation with composition in the blends.

a small amount of PMMAEA had not enough effect on the plasticization of the PMMAEA/PMMA system in the melting zone. Increasing PMMAEA weight percent, the PMMAEA/PMMA system took less time to plasticize in the melting zone, leading to lower $\bar{t}$.

To characterize the quality of the axial mixing along the barrel of the TSE for the three systems, the Peclet number, *Pe*, is presented in Figure 8(c) as a function of blends composition. A decrease in the *Pe* number means an increase in the axial mixing intensity. For the SMA8/PS system, *Pe* curve (square symbols) shows a positive deviation from the linear additivity rule, which is an indication of a weaker axial mixing of SMA8/PS system compared with that of pure SMA8 and PS phases. On the contrary, SMA14/SAN17 system shows a negative deviation from the linear additivity rule, which indicate a better axial mixing of the SMA14/SAN17 system compared with that of pure SMA14 and SAN17 phases. *Pe* number for the PMMAEA/PMMA system is approximately constant (i.e., independent on system composition). This indicates that, under the same processing conditions, the mixing quality of the PMMAEA/PMMA system is identical to that of its pure components.

CONCLUSIONS

In this experimental study, we studied the RTD behavior of pure polymers and miscible or immiscible polymer/polymer systems in a corotating TSE using a fluorescence monitoring device installed at the extruder die. The RTD characterization was performed under the same screw configuration, constant RPM, feeding rate, and temperature profile. Under these constant processing conditions, a good linearity between the amplitude of the fluorescence signal measured at the TSE die and the amount of the tracer incorporated at the main hopper was observed. Depending on their viscosities and the corresponding pressures generated at the TSE die, it was observed that polymers presenting higher viscosity or higher pressure showed longer residence time along the TSE barrel, and consequently led to a better axial mixing.

The RTD behavior of three binary polymer blends (two miscible and one immiscible) were characterized in terms of the mean residence time, peak of fluorescence intensity, and Peclet number. For the miscible systems (SMA14/SAN17 and PMMAEA/PMMA), the mean residence time and fluorescence peak intensity showed a linear variation between those of the pure blend components. The Peclet number, a measure of the level of axial mixing along the barrel of the TSE, showed a negative deviation from the additivity rule for SMA14/SAN17 system (higher axial mixing intensity than the pure SMA14 and SAN17 components) and remained constant for PMMAEA/PMMA (the same axial mixing intensity than the pure PMMAEA and PMMA components). However, for the immiscible SMA8/PS system, the mean residence time was between those of pure SMA8 and PS phases but closer to that of SMA8. This was attributed to the preferential localization of the tracer inside the SMA8 phase, consequently monitoring only the flowing behavior of this phase along the TSE.

References

1. Bur, A. J.; Gallant, F. M. Polym Eng Sci 1991, 31, 1365.
2. Carneiro, O. S.; Covas, J. A.; Ferreira, J. A.; Cerqueira, M. F. Polym Test 2004, 23, 925; and references cited therein.
3. Hu, G. H.; Kadri, I. Polym Eng Sci 1999, 39, 930.
4. Hu, G. H.; Kadri,I Polym Eng Sci 1999, 39, 299.
5. Hu, G. H.; Sun, Y. J.; Lambla, M. J Appl Polym Sci 1996, 61, 1039.
6. Poulesquen, A.; Vergnes, B.; Cassagnau, P.; Michel, A.; Carneiro, O. S.; Covas, J. A. Polym Eng Sci 2003, 43, 1849.
7. Xu, Z. B.; Feng, L. F.; Hu, G. H.; Song X. B.; Zhang, X. M.; Li, G. Z.; Gu, X. P.; Li, B. G. Plast Rubber Compos 2006, 35, 439.
8. Cassagnau, P.; Mijangos, C.; Michel, A. Polym Eng Sci 1991, 31, 772.
9. Lappe, H.; Potente, H. SPE ANTEC Tech Papers 1984, 305, 108.
10. Weiss, R. A.; Stamato, H. Polym Eng Sci 1989, 29, 134.
11. Kadri, I. Ph.D. Thesis, Etude de la Distribution des Temps de Séjour dans une Extrudeuse Bivis Corotative, Université Louis Pasteur de Strasbourg: France, 1997.
12. Kim, P. J.; White, J. L. Int Polym Proc 1994, 9, 108.
13. Polance, R.; Jayaraman, K. Polym Eng Sci 1995, 35, 1535.
14. Elkouss, P.; Bigio, D. I.; Wetzel, M. D.; Raghavan, S. R. AIChE J 2006, 52, 1451.
15. Kao, S. V.; Allison, G. R. Polym Eng Sci 1984, 24, 645.
16. Tzoganakis, C.; Tang, Y.; Vlachopoulos, J.; Hamielec, A. E. J Appl Polym Sci 1989, 37, 681.
17. Zhang, X. M.; Feng, L. F.; Hoppe, S.; Hu, G. H. Polym Eng Sci 2006, 46, 510.
18. Zhang, X. M.; Feng, L. F.; Hoppe, S.; Hu, G. H. Polym Eng Sci 2008, 48, 19.
19. Cassagnau, P.; Coumont, M.; Melis, F.; Puaux, J. P. Polym Eng Sci 2005, 45, 926.
20. Mélo, T. J. A.; Canevarolo, S. V. Polym Eng Sci 2005, 45, 11.
21. Levenspiel, O. Chemical Reaction Engineering, 2nd ed.; Wiley: New York, 1972.
22. Todd, D. B. Polym Eng Sci 1975, 15, 437.
23. Gao, J,;Walsh, G. C.; Bigio, D.; Briber, R. M.; Wetzel, M. D. AIChE J 1999, 45, 2541.
24. Gao, J; Walsh, G. C.; Bigio, D.; Briber R. M.; Wetzel, M. D. Polym Eng Sci 2000, 40, 227.
25. Martinez, F.; Neculqueo, G.; Torres, M. A. Olea Bol Soc Chil Quím 2001, 46, 137.
26. Lee, S. M.; Park, J. C.; Lee, S. M.; Ahn, Y. J.; Lee J. W. Korea-Austria Rheol J 2005, 17, 87.
27. Chen, T.; Patterson, W. I.; Dealy, J. M. Int Polym Proc 1995, 10, 3.
28. Bikiaris, D.; Prinos, J.; Botev, M.; Betchev, C.; Panayiotou, C. J Appl Polym Sci 2004, 93, 726.
29. Gan, P. P.; Paul, D. R. J Appl Polym Sci 1994, 54, 317.
30. Kim, J. H.; Barlow, J. W.; Paul, D. R. J Polym Sci Part B: Polym Phys 1989, 27, 223.
31. Brannock, G. R.; Barlow, J. W.; Paul, D. R. J Polym Sci Part B: Polym Phys 1991, 29, 413.
32. Fang, H. X.; Mighri, F.; Ajji, A. J Appl Polym Sci 2007, 105, 2955.